J|A|C|S COMMUNICATIONS

Published on Web 05/11/2009

Synthetic Haggite $V_4O_6(OH)_4$ Nanobelts: Oxyhydroxide as a New Catalog of Smart Electrical Switch Materials

Changzheng Wu, Jun Dai, Xiaodong Zhang, Jinlong Yang, and Yi Xie*

Hefei National Laboratory for Physical Sciences at Microscale, University of Science & Technology of China, Hefei, Anhui 230026, P.R. China

Received March 19, 2009; E-mail: yxie@ustc.edu.cn

Metal(semiconductor)−insulator transitions (MIT) accompanied by huge temperature-induced resistivity changes as well as selectively optical switches received much attention during the past decades for the construction of intelligent devices such as electrically driven Mott field-effect transistors, temperature sensors, and energy-efficient smart windows.[1] Generally, the well-known MIT materials only include two main categories of oxides (V_nO_{2n-1}, $MNiO_3$, Sr_2RuO_4, Ti_2O_3, Fe_3O_4, etc.) and sulfides ($BaVS_3$, NiS, $NiS_{2-x}Se_x$, etc.).[2]

Currently, atomic structural analysis gave us inspiration that oxyhydroxide haggite $V_4O_6(OH)_4$ would be a new catalog of MIT material. For the haggite phase, it consists of double octahedron chains linked by an octahedron corner to form the corrugated sheets that are parallel to the (001) plane.[3] Moreover, the presence of infinite V−V chains in haggite along the *b*-axis with the nearest V−V distances of 0.299 nm (Figure 1) inspired us to further pursue its potential physical properties due to its structural similarity with tetragonal rutile VO_2 (metallic phase) for the characteristic of infinite vanadium atom chains. For the transformation of rutile to monoclinic VO_2, with the driving force of decreased temperature, the small distortion of infinitely linear V−V chains in rutile VO_2 to form zigzag vanadium-atom chains in monoclinic VO_2[4] accounts for the occurrence of metal−insulator transition (Figure S1). Analogously, haggite is particularly attractive for potential electrical transitions due to the presence of infinitely linear V−V chains similar to those in rutile VO_2. Therefore, haggite has more promising temperature-driven switch properties and represents a new catalog of oxyhydroxide MIT materials.

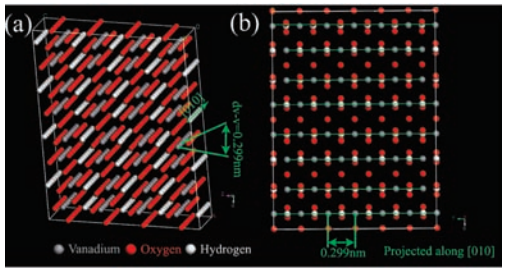

Figure 1. (a) Atomic supercell structure of haggite $V_4O_6(OH)_4$ projected along a random direction, from which the linear vanadium atoms could be clearly seen. (b) Supercell structure of orthorhombic haggite $V_4O_6(OH)_4$ projected along [010] and the vanadium atom built chains parallel to the *b* axis of the haggite structure.

However, although haggite mineral was discovered from the Colorado Plateaus region in the 1950s,[3] it has been significantly neglected ever since, while in the past decades the chemical and physical information of haggite only comes from its mineral sample due to the absence of a chemically synthetic sample. Herein, we highlight an available pathway to accomplish the challenge by a controlled oxidation reaction of $V(OH)_2NH_2$ in a formic acid (HCOOH) buffer solution, representing the first synthetic case for a haggite phase. The XRD reflection of the synthetic product (Figure S2) matches well with that of standard JCPDS card No.74-1688, corresponding to haggite $V_4O_4(OH)_6$ with the space group $C_{2/m}$. And the calculated XRD pattern from the haggite crystal cell is identical to the experimental pattern, providing direct evidence for the haggite phase of the synthesized product.

However, although haggite has a definite position for vanadium, oxygen, and hydrogen atoms (Figure 2a) with a given space group of $C_{2/m}$ by Evans and Mrose,[3] the symmetry equivalence of hydrogen atoms seems to be ignored in that case. Our careful analysis clarified the formula of haggite as $V_4O_6(OH)_4$, rather than $V_4O_4(OH)_6$, due to the presence of four hydrogen atoms that are face shared by two neighbored unit cells (Figure S2).

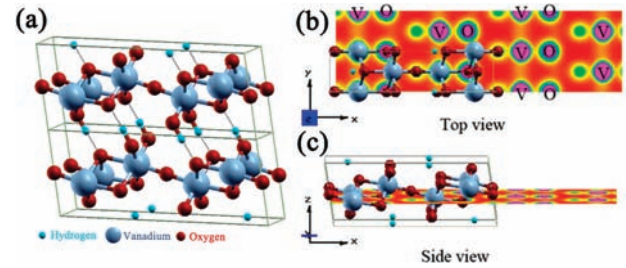

Figure 2. (a) Supercell structure (1 × 1 × 2) of haggite. Top view (b) and side view (c) of the charge density of a selected vanadium-atom plane for a 2 × 2 × 1 haggite super cell.

Moreover, since the valence for all the vanadium ions in $V_4O_6(OH)_4$ should be +4 while the $V_4O_4(OH)_6$ should have a mixture of a 1:1 ratio of V^{3+} and V^{4+}, the vanadium valence of as-obtained haggite product by theoretical and experimental analysis then provides another clue to determine the number of hydrogen atoms in haggite. First, in haggite all the vanadium atoms have the same valence based on the theoretical calculation of charge density. The top view of valence charge contour plot for a 2 × 2 × 1 super cell was shown in Figure 2b, while the corresponding atomic localization for vanadium and oxygen atoms were discerned by a side view plot (Figure 2c), where all the vanadium atoms have the same color scope with the same charge value of 10.7577 (e) (Table S1), revealing uniform vanadium valence in haggite. Second, direct experimental information for the valence state of vanadium ions is further provided by the analysis of the surface molecular and electronic structure of the products by XPS (Figure S3), as well as the redox titration results. They both experimentally verified that all the vanadium atoms in haggite have a uniform valence state of +4, thus rationalizing the formula $V_4O_6(OH)_4$ for haggite.

TEM and FE-SEM images (Figure S4−5) show the nanobelt morphology with width ranging from 100 to 400 nm, lengths up to hundreds of micrometers, and the thickness of nanobelts being 10−40 nm, in which the preferred crystallographic orientation of

10.1021/ja9020217 CCC: $40.75

nanobelts is along the [110] direction. Also, the orientation angle value of 87.9° between (110) and (001) is fairly consistent with that calculated from monoclinic crystallographic parameters of haggite $V_4O_6(OH)_4$ (88.0°), providing further evidence for haggite $V_4O_6(OH)_4$. In our case, the nanobelt structure and observed crystallographic orientations mirror the internal crystal structure of haggite $V_4O_6(OH)_4$. The fact that the average longest and relatively shorter V−O bonds were along the [001] and [110] directions, respectively, reveals that the [110] direction has a relatively high stacking rate, enabling fast growth along the [110] axis (Figure S5). Actually, the relative stacking rates of the octahedron at various crystal faces answer for the growth direction of haggite nanobelts.

Haggite is theoretically and experimentally found to be a semiconductor with a small band gap of 1.4 eV. As is known, the critical separation distance for electrons itinerant or localized in a crystal structure answers for the strength of the V−V coupling interaction between 3d electrons of neighboring atoms with a distance value of 2.94 Å for a V^{4+}−V^{4+} ion.[5] In our haggite case, the nearest distance (2.99 Å) for neighboring V^{4+}−V^{4+} in the infinite chains is slightly larger than this critical distance, implying the electron clouds of vanadium atoms could not overlap each other in the infinite V^{4+}−V^{4+} chains to form metallic behavior, resulting in it being a semiconductor. Also, the UV−vis spectrum gives further information for semiconductivity for the as-obtained haggite with an accepted band gap value of 1.4 eV (Figure S6). The first-principle calculation (LSDA + U method [6]) with an effective orbital potential value of $U_{\mathrm{eff}} = 4$ eV for V 3d electrons also yields the semiconducting ground state (S4), in agreement with the experimental band gap results.

As is shown in Figure 3a, in the high temperature range, the resistivity is relatively low, and it shows the increase of electrical resistivity as the temperature decreases with $d\rho/dT < 0$ (Figure S7), behaving similarly to the semiconductor character[7] of the synthetic haggite. Below 100 K, the resistivity rapidly increases by $>10^4$ orders of magnitude down to the low temperature studied with an inflection point at 66.6 K (inset in Figure 3a). The abrupt increase at 66.6 K gives direct evidence for a transition from the small-gap semiconductor at higher temperature to an insulator at lower temperature.

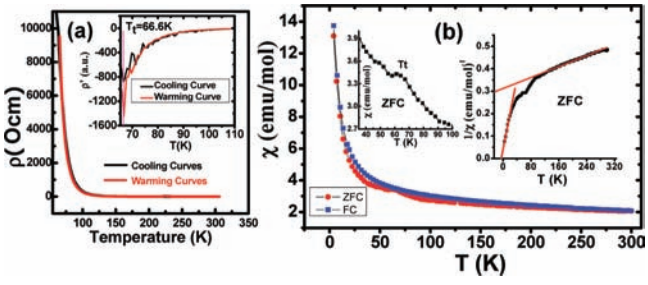

Figure 3. (a) Temperature dependence of the resistivity of the synthetic haggite sample. Inset: the differential resistivity versus temperature (T) plot in the temperature range <110 K. (b) ZFC and FC magnetization measured as a function of temperature (4 to 300 K). Inset: left part is the magnified part for ZFC curves, where the temperature Tt of the semiconductor−insulator transition was indexed; right part is inverse susceptibility $\chi^{-1}(T)$ of synthetic haggite with best linear fits according to the Curie−Weiss law.

The curves of magnetic susceptibility dependent on temperature show an anomaly jump of the magnetic susceptibility at ∼66 K (Transition temperature, Tt), showing the magnetic response for the semiconductor−insulator transition. Furthermore, the straight lines in the right side inset in Figure 3b are the best fits for the Curie−Weiss law $\chi(T) = \chi_0 + C/(T - \theta)$[8] above 100 K and below 40 K. From the linear extrapolation of the high temperature part of the susceptibility curves, a negative extrapolated Curie−Weiss temperature ($\theta = -517$ K) can be obtained, indicative of the presence of a strong antiferromagnetic interaction between V ions in the haggite sample. The change of magnetic susceptibility in the range 40−100 K, as well as the distinct Curie−Weiss temperatures of −517 and −12.6 K for the high temperature and low temperature magnetic phases, respectively, clearly reveals that a magnetic phase transition takes place accompanied by structural changes. In our case, due to the presence of vanadium ion chains similar to those in metallic VO_2, for the haggite case, the characteristic feature of charge localization occurs due to pairing of vanadium ions, and some of these pairs have a spin-singlet ground state.[9] Thus, the electrons in the high-temperature semiconductor are much more localized to form an insulator at lower temperature, accompanied by the changes in magnetic properties, leading to the semiconductor−insulator transition of oxyhydroxide haggite.

In conclusion, synthetic haggite $V_4O_6(OH)_4$ has been successfully obtained for the first time after a delay of more than 50 years. Our careful analysis clarifies the formula of haggite as $V_4O_6(OH)_4$, rather than the long-standing known $V_4O_4(OH)_6$. The semiconductor of haggite shows a rapid increase of resistance by $>10^4$ orders of magnitude down to low temperatures, giving the first case of the oxyhydroxide compound showing semiconductor−insulator transitions. More intriguingly, the haggite product's nanobelt that can act as connecting units have potential in the construction of intelligent switching devices in future investigations.

Acknowledgment. This work was financially supported by National Basic Research Program of China (No. 2009CB939901), National Natural Science Foundation of China (No.20621061, 20801051), and China Postdoctoral Science Foundation funded project (200801235, 20080430102). Also this research is supported by the Shanghai Supercomputer Center.

Supporting Information Available: Structural analysis of rutile and monoclinic VO_2, experimental procedures, supplemental calculation data, XPS spectra, TEM and SEM images of haggite nanobelts and their structural mechanism, bandgap analysis and the crystallographic information file for synthetic haggite product. This material is available free of charge via the Internet at http://pubs.acs.org.

References

(1) (a) Qazilbash, M. M.; Brehm, M.; Chae, B. G.; Ho, P. C.; Andreev, G. O.; Kim, B. J.; Yun, S. J.; Balatsky, A. V.; Maple, M. B.; Keilmann, F.; Kim, H. T.; Basov, D. N. *Science* **2007**, *318*, 1750. (b) Guiton, B. S.; Gu, Q.; Prieto, A. L.; Gudiksen, M. S.; Park, H. K. *J. Am. Chem. Soc.* **2005**, *127*, 498. (c) Jaroszynski, J.; Popovic, D. *Phys. Rev. Lett.* **2007**, *99*, 216401.
(2) (a) Imada, M.; Fujimori, A.; Tokura, Y. *Rev. Mod Phys.* **1998**, *70*, 1039, and references therein. (b) Baum, P.; Yang, D. S.; Zewail, A. H. *Science* **2007**, *318*, 788.
(3) Evans, H. T.; Mrose, M. E. *Acta Crystallogr.* **1958**, *11*, 56.
(4) Biermann, S.; Poteryaev, A.; Lichtenstein, A. I.; Georges, A. *Phys. Rev. Lett.* **2005**, *94*, 026404.
(5) (a) Djerdj, I.; Sheptyakov, D.; Gozzo, F.; Arcon, D.; Nesper, R.; Niederberger, M. *J. Am. Chem. Soc.* **2008**, *130*, 11364. (b) Goodenough, J. B. *J. Solid. State. Chem.* **1971**, *3*, 490.
(6) (a) Sheng, H. W.; Liu, H. Z.; Cheng, Y. Q.; Wen, J.; Lee, P. L.; Luo, W. K.; Shastri, S. D.; Ma1, E. *Nat. Mater.* **2007**, *6*, 192. (b) Vinh, H. T.; Miiller, W.; Bukowski, Z. *Phys. Rev. Lett.* **2008**, *100*, 137004. (c) Fennie, C. J.; Rabe, K. M. *Phys. Rev. Lett.* **2006**, *96*, 205505.
(7) (a) Tenga, A.; Lidin, S.; Belieres, J. P.; Newman, N.; Wu, J.; Haussermann, U. *J. Am. Chem. Soc.* **2008**, *130*, 15564. (b) Huang, F. Q.; Brazis, P.; Kannewurf, C. R.; Ibers, J. A. *J. Am. Chem. Soc.* **2000**, *122*, 80.
(8) (a) Ashley, A. E.; Cooper, R. T.; Wildgoose, G. C.; Green, J. C.; O'Hare, D. *J. Am. Chem. Soc.* **2008**, *130*, 15662. (b) Nelson, J. A.; Bennett, L. H.; Wagner, M. J. *J. Am. Chem. Soc.* **2002**, *124*, 2979.
(9) Park, J.; Oh, I. H.; Lee, E.; Lee, K. W.; Lee, C. E.; Song, K.; Kim, Y. J. *Appl. Phys. Lett.* **2007**, *91*, 153112.

JA9020217